[CANCER RESEARCH 64, 3731–3736, June 1, 2004]

*Advances in Brief*

# Vascular Normalization by Vascular Endothelial Growth Factor Receptor 2 Blockade Induces a Pressure Gradient Across the Vasculature and Improves Drug Penetration in Tumors

**Ricky T. Tong,[1,2] Yves Boucher,[1] Sergey V. Kozin,[1] Frank Winkler,[1] Daniel J. Hicklin,[3] and Rakesh K. Jain[1]**

*[1]E. L. Steele Laboratory for Tumor Biology, Department of Radiation Oncology, Massachusetts General Hospital and Harvard Medical School, Boston, Massachusetts; [2]The Harvard-Massachusetts Institute of Technology Division of Health Sciences and Technology, Cambridge, Massachusetts; and [3]ImClone Systems, Incorporated, New York, New York*

## Abstract

**Elevated interstitial fluid pressure, a hallmark of solid tumors, can compromise the delivery of therapeutics to tumors. Here we show that blocking vascular endothelial growth factor (VEGF) signaling by DC101 (a VEGF-receptor-2 antibody) decreases interstitial fluid pressure, not by restoring lymphatic function, but by producing a morphologically and functionally "normalized" vascular network. We demonstrate that the normalization process prunes immature vessels and improves the integrity and function of the remaining vasculature by enhancing the perivascular cell and basement membrane coverage. We also show that DC101 induces a hydrostatic pressure gradient across the vascular wall, which leads to a deeper penetration of molecules into tumors. Thus, vascular normalization may contribute to the improved survival rates in tumor-bearing animals and in colorectal carcinoma patients treated with an anti-VEGF antibody in combination with cytotoxic therapies.**

## Introduction

The present treatment of solid tumors is plagued by two problems: physiological barriers impair the delivery of therapeutic agents in optimal quantities, and genetic and epigenetic mechanisms contribute to drug resistance. Antiangiogenic therapy has the potential to overcome or circumvent these problems. A recent Phase III clinical trial (1) has provided the first clinical proof of this hypothesis, the combination of Avastin, a monoclonal antibody against vascular endothelial growth factor (VEGF), with conventional chemotherapy increased disease-free survival by 5 months in colorectal cancer patients. In addition to the direct antivascular effects that lead to the death of cancer cells, we proposed that anti-VEGF antibody improves the delivery of cytotoxic agents to tumors and, thus, increases the effectiveness of combination therapy (2). We have recently shown that an anti-VEGF antibody can lower interstitial fluid pressure (IFP) in transplanted tumors in mice (3) and in rectal carcinomas in patients (4). However, the mechanisms of IFP reduction and how this reduction affects drug delivery are not known. In normal tissues, the excess fluid filtered from blood vessels is drained by lymphatic vessels to maintain the IFP close to zero (mm Hg). In tumors, IFP homeostasis is perturbed because of impaired lymphatic function (5, 6) and abnormalities in vascular structure and function (7). Because of the high vascular permeability and the impaired lymphatic drainage, the oncotic and hydrostatic pressures in the microvascular and interstitial spaces are at equilibrium in tumors (8, 9). To unravel the mechanism of IFP reduction induced by blocking VEGF signaling, we examined the effect of DC101 on the determinants of interstitial hypertension, including changes in the morphology, wall structure, and function of tumor vasculature during the course of treatment.

Received 1/9/04; revised 3/18/04; accepted 4/9/04.

**Grant support:** Supported in part by National Cancer Institute Grant P01-CA-80124. R. Tong received graduate fellowships from the National Science Foundation and Susan G. Komen Breast Cancer Foundation.

The costs of publication of this article were defrayed in part by the payment of page charges. This article must therefore be hereby marked *advertisement* in accordance with 18 U.S.C. Section 1734 solely to indicate this fact.

**Requests for reprints:** Rakesh Jain, E. L. Steele Laboratory for Tumor Biology, Department of Radiation Oncology, COX 734, Massachusetts General Hospital, 100 Blossom Street, Boston, MA 02114. Phone: (617) 501-4083; Fax: (617) 724-1819; E-mail: jain@steele.mgh.harvard.edu.

## Materials and Methods

**Animals and Tumors.** The murine mammary carcinoma MCaIV, human small cell lung carcinoma 54A, human glioblastoma multiforme U87, and human colon adenocarcinoma LS174T were grown in nude or severe combined immunodeficient (SCID) mice. MCaIV, 54A, and U87 were transplanted s.c. MCaIV and LS174T tumors were also transplanted in dorsal skinfold chambers in SCID mice for intravital microscopy and for microvascular pressure (MVP) and IFP measurements. Animals were anesthetized with ketamine/xylazine (100/10 mg/kg, i.m.) unless otherwise noted.

**DC101 Treatment.** DC101 (ImClone Systems Inc., New York, NY) was administered i.p. at a dose of 40 mg/kg, previously determined to have antitumor effects *in vivo* (10). The control group received 40 mg/kg, i.p of nonspecific rat IgG1 antibody (ImClone). All of the experiments were done 3 days after the injection of DC101 (IgG for the control), unless otherwise noted.

**Functional Lymphatic Assay.** To identify the functional lymphatic vessels in tumors, ferritin microlymphangiography and lymphatic vessel endothelial hyaluronan receptor-1 (LYVE-1) immunostaining were performed according to published methods (6).

**Intravital Microscopy.** To visualize functional blood vessels in MCaIV or LS174T in the dorsal chamber of SCID mice *in vivo*, fluorescein-labeled dextran ($M_r$ 2,000,000; Sigma) was injected i.v. (11). Vascular length per unit area and vessel mean diameter were obtained by averaging measurements over six random regions per mouse. The effective vascular permeability was measured using cyanine-5-labeled BSA as described previously (12). For multiphoton microscopy images, maximum intensity projections of stacked images were done offline using Confocal Assistant.

**Immunostaining of Collagen IV.** MCaIV-tumor-bearing mice ($n = 6$ in control group; $n = 5$ in DC101-treated group) were injected with FITC-CD31 1 h before perfusing fixative. The mice were perfused and fixed with 4% paraformaldehyde, and 100-$\mu$m-thick sections were prepared (13). Collagen IV (Chemicon) was stained overnight; and tetramethyl rhodamine isothiocyanate (TRITC) goat antirabbit antibody was used as a secondary antibody. Three images per section were taken by confocal microscopy. Total vessel length and the length of segments covered by collagen IV were traced in three random regions (each region was 700 $\mu$m by 700 $\mu$m) for each 100-$\mu$m-thick section. On average, ~50 vessel segments were measured per mouse.

**Immunostaining of *αSMA*.** Similarly, MCaIV-tumor-bearing mice ($n = 4$) were given injections of FITC-CD31 and were perfused and fixed with 4% paraformaldehyde, and 100-$\mu$m-thick sections were prepared. Anti-$\alpha$-smooth muscle actin ($\alpha$SMA; Cy-3-conjugated mouse monoclonal, clone 1A4; Sigma) antibody was used to identify $\alpha$SMA-positive perivascular cells. The tissue sections were examined using a confocal microscope. Quantification was performed in a manner similar to collagen IV staining.

**IFP Measurements with the Wick-in-Needle Technique.** IFP was measured with the wick-in-needle technique (14) prior to and during DC101/control

antibody treatment for 54A and U87. DC101/control antibodies were injected once every 3 days. For each time point, IFP was measured in at least two different tumor regions.

**MVP and IFP Measurements with the Micropipette Technique.** MCaIV tumors were implanted in the dorsal skinfold chamber of SCID mice as described previously (15). The dorsal skinfold chamber preparation provides a stable and easy access for IFP and MVP measurements with the micropipette technique (8, 16). For each mouse, two to seven IFP and MVP measurements were obtained. Under stereomicroscopic guidance, micropipettes with an opening of ~2.5 $\mu$m were inserted inside blood vessels to measure the MVP (confirmed by Lissamine Green B injection). The IFPs were generally measured at 0.5–1 mm from the tumor surface.

**Oncotic Pressure Measurements.** The chronic wick technique was used to collect tumor interstitial fluid (9). A long wick (~5 cm) was transplanted together with the MCaIV tumors and was collected postmortem 2 weeks later; interstitial fluid was obtained by centrifugation. A membrane colloid osmometer with ultrafiltration membranes (Amicon PM10; Millipore Corp., Bedford, MA) was used to measure oncotic pressure.

**Extravasation of TRITC-BSA.** TRITC-BSA (0.1 ml; Molecular Probes) was injected i.v. 1 h before perfusion fixation in tumor-bearing mice. Biotinylated lectin was also injected 5 min before fixation. Three 10-$\mu$m-thick frozen sections, 50 $\mu$m apart, were prepared from each tumor block. Images were taken using two-photon microscopy. Perfused biotinylated lectin was used to identify functional vessels, and extravasation pattern of TRITC-BSA was analyzed using a program written in ImageJ. Ten concentric rings of 3.25-$\mu$m thickness were drawn starting at the vessel wall. Average intensity was calculated within each ring, and the intensity profile was fitted to an exponential function ($I = Ae^{-x/L} + C$, where I = pixel intensity, $x$ = distance from vessels, and $L$ = characteristic penetration length). The characteristic penetration length was compared between the two treatment groups.

**Statistical Analysis.** Data are presented as mean ± SE. Significant differences between groups were determined with a Student's $t$ test (JMP Program). $P < 0.05$ was considered statistically significant.

## Results

**DC101 Decreases IFP without Affecting Lymphatic Function.** We first confirmed that similar to a VEGF blocking antibody (3), DC101 decreased IFP in both human small cell lung carcinoma 54A (Fig. 1*A*), and human glioblastoma multiforme U87 xenografts (Fig. 1*B*). At the same time, we did not find any evidence of functional lymphatic vessels in the tumors of either treated or control animals (Fig. 1*C*). Thus, the drop in IFP could not be attributed to modifications in lymphatic function.

**DC101 Normalizes the Architecture of the Tumor Vasculature.** We then examined the effect of DC101 on the morphology of blood vessels in the murine mammary carcinoma MCaIV growing in dorsal skinfold chambers. Three days after a single injection of DC101, the vascular density and vessel diameter decreased significantly (Table 1; Fig. 2, *A* and *B*). To obtain further insight into the dynamic changes occurring in the tumor vasculature, we continuously monitored the same region of the tumor over 6 consecutive days using two-photon microscopy. This technique allowed us to image up to 200 $\mu$m deep with 1-$\mu$m resolution (11). In contrast to skeletal muscle, which has an organized vasculature with a relatively smooth vascular wall and uniform diameter (Fig. 2*C*), untreated MCaIV tumors had tortuous vessels with abrupt changes in vessel diameter (*arrowheads* in Fig. 2*D*). On the basis of the dynamic high resolution images, the surprising finding was that, 2–3 days after DC101 treatment, many of these vessels also became less tortuous besides getting smaller in diameter (*arrow* in Fig. 2*E*). By day 5, in some regions, some of these vessels regressed completely. Furthermore, the vessels at the tumor–host interface also became less tortuous and assumed a relatively normal morphology (Fig. 2*F*). Similar striking vascular changes were also observed in the human colon adenocarcinoma LS174T (Fig. 2, *G* and *H*). Thus, DC101 "normalizes" the architecture of the vascular network before complete regression.

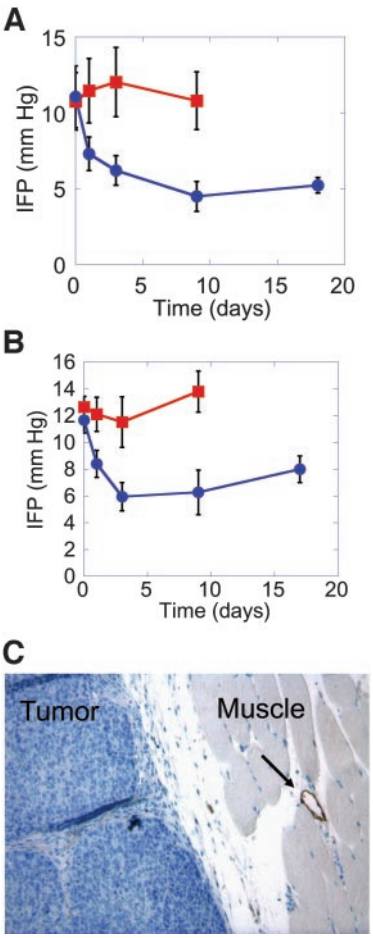


Fig. 1. DC101 decreased the interstitial fluid pressure (IFP) in multiple tumor models without affecting lymphatic function. *A* and *B*, ■, the control group; ●, the DC101 group. DC101 lowered the IFP in 54A tumors (*A*) and in U87 tumors (*B*) implanted s.c. in nude mice. Data are represented as mean ± SE. *C*, a lymphatic vessel endothelial hyaluronan receptor-1 (LYVE-1)-positive lymphatic vessel in the skeletal muscle adjacent to a MCaIV tumor (*arrow*). No LYVE-1-positive vessels were found inside the tumor in either the DC101 or the control group.

**DC101 Normalizes the Wall Structure of the Tumor Vasculature.** In addition to architectural abnormalities, the tumor vasculature is characterized by a paucity of, or abnormalities in, mural cells and basement membrane (7, 13, 17). To test whether DC101 also normalized the wall structure, we perfused the tumors with FITC-CD31 and stained frozen sections for collagen IV and $\alpha$SMA (which label basement membrane and mural cells, respectively). Unlike the vessels in normal muscle, the collagen IV staining around some vessels was below the detection limit in MCaIV tumors (Fig. 3*A*). Consistent with normalization, more vessels exhibited collagen IV staining after DC101 treatment (Fig. 3, *B* and *C*). DC101 also significantly increased the fractional coverage of tumor blood vessels by $\alpha$SMA-positive cells (Fig. 3*D*). Approximately 25% of the vessels in untreated tumors had little or no perivascular cell coverage, but this fraction dropped to ~8% after DC101 treatment ($P < 0.005$). Thus, DC101 induces structural normalization of the tumor vasculature by homogenizing the vessel size, reducing vessel tortuosity, and increasing the fractional coverage of the vascular endothelium by perivascular cells and basement membrane.

**DC101 Enhances Oncotic Pressure Gradient Across the Tumor Vasculature.** To determine whether structural normalization of tumor vessels translates into functional normalization, we measured the

Table 1 *Physiological changes in tumor vasculature after DC101 treatment*

Vascular morphology and permeability were measured before and 3 days after a single injection of DC101/control antibodies. No changes were observed for the control group. DC101 significantly reduced the vascular density, diameter, and vascular permeability in MCaIV tumors implanted in dorsal skinfold chambers of severe combined immunodeficient (SCID) mice *versus* control. Data are represented as mean ± SE ($n = 5$).

| | Control group | | DC101 group | |
|---|---|---|---|---|
| | Before | After | Before | After |
| Vascular length per unit area, cm/cm$^2$ | 62.0 ± 2.8 | 52.1 ± 4.6 | 58.8 ± 2.2 | 41.9 ± 3.0[a] |
| Vessel diameter, $\mu$m | 49.8 ± 5.1 | 54.4 ± 4.4 | 51.1 ± 3.7 | 32.2 ± 4.0[b] |
| Vascular permeability, $10^{-7}$ cm/s | 6.81 ± 1.24 | 7.31 ± 0.77 | 5.78 ± 0.65 | 2.79 ± 0.78[c] |

[a] $P < 0.005$.
[b] $P < 0.01$.
[c] $P < 0.05$.

functional parameters that govern the transport of molecules across the vessel wall. These include vascular permeability, plasma and interstitial oncotic pressures, MVP, and IFP (18, 19). Three days after the injection of DC101 the vascular permeability of albumin in MCaIV, a profoundly leaky tumor, was decreased by 51% (Table 1). In general, leaky vessels in tumors lead to an increase in the interstitial oncotic pressure (9), which becomes approximately equal to the plasma oncotic pressure. We found that in DC101-treated tumors the interstitial oncotic pressure was significantly lower than in the control group (Fig. 3*E*), whereas the plasma oncotic pressure did not change. This decrease in interstitial oncotic pressure is consistent with the decrease in vascular permeability to macromolecules induced by DC101. The enhanced oncotic pressure gradient across the vasculature is another hallmark of tumor vasculature normalization.

**DC101 Induces a Hydrostatic Pressure Gradient Across the Tumor Vasculature.** In solid tumors, MVP is approximately equal to IFP, leading to nearly zero pressure difference across the vessel wall (8). As a matter of fact, these two pressures are so closely coupled that changing the vascular pressure leads to similar changes in the IFP within seconds, until they both become equal again (20). Thus the

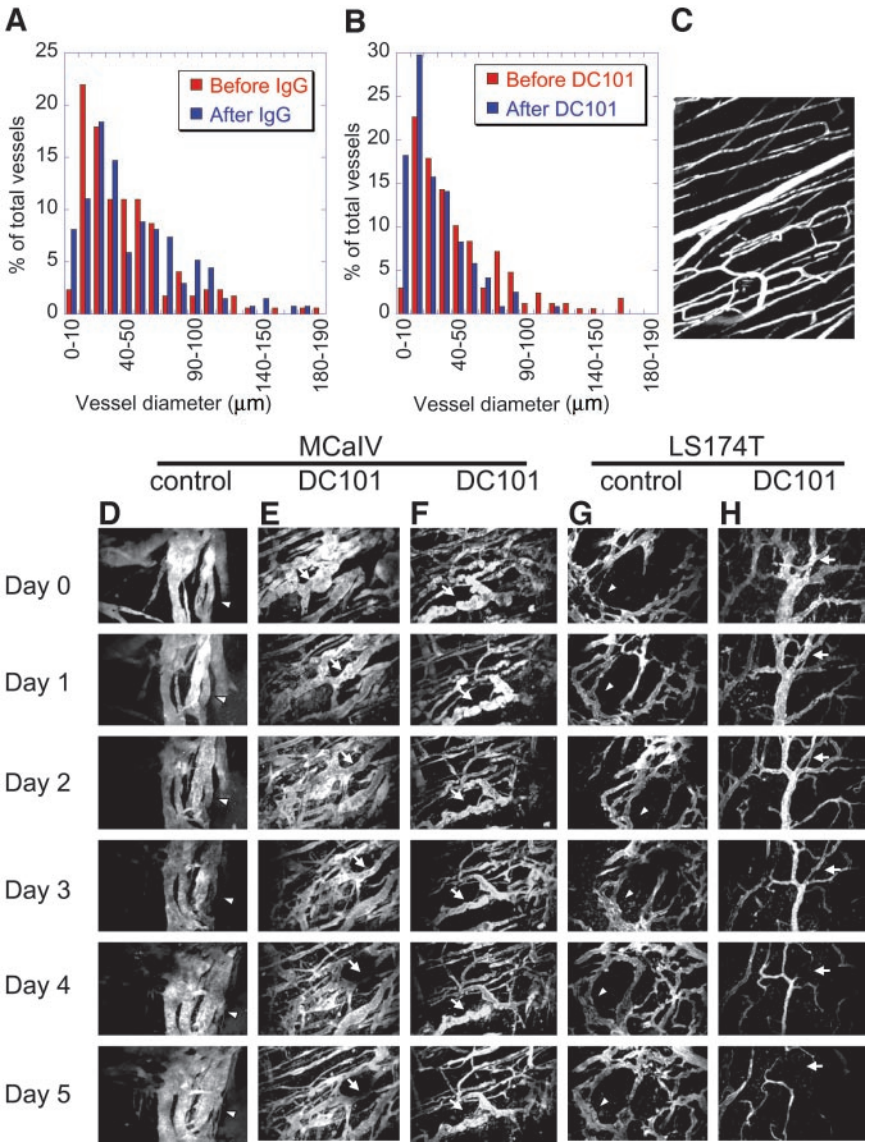


Fig. 2. Dynamics of DC101-induced vessel normalization. Vessel diameters before and 3 days after control IgG (*A*) or DC101 (*B*) treatment. DC101 significantly altered the distribution of vessel diameters (F test. $P < 0.0001$). *C*, two-photon image showing normal skeletal muscle blood vessels. Daily images of the same MCaIV tumor vessels in the control (*D*) and DC101 (*E*) groups were taken over a period of 6 days with a two-photon microscope. *F*, DC101 normalized vessels at the MCaIV tumor margin. Similar results were observed in LS174T tumors in the control (*G*) and DC101 (*H*) groups. For each control group, some vessels disappeared, but the caliber of most vessels did not change or decrease in size (*arrowheads* in *D* and *G*). In contrast, in DC101-treated mice, many tumor vessels were either pruned or reduced in size (*arrows* in *E*, *F*, and *H*). Some vessels appeared less tortuous after DC101 treatment. Image width: *C*, 250 $\mu$m; *D–H*, 500 $\mu$m. DC101/control antibodies (40 mg/kg) were injected on day 0 and day 3.

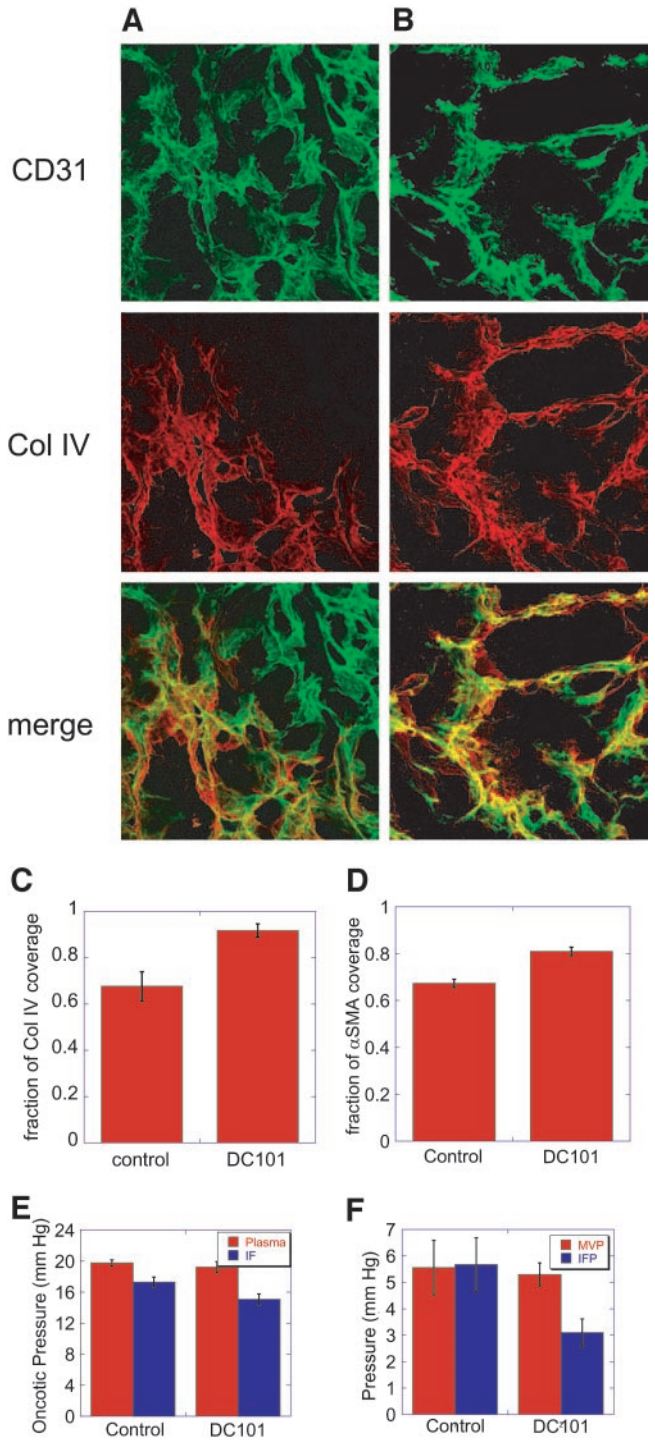


Fig. 3. Normalization of vessel wall by DC101. Vessels were perfused with FITC-CD31 (*green*) and basement membrane was stained with collagen IV-specific antibody (*red*). *A*, in the control MCaIV tumors, some vessels lacked collagen IV staining (*Col IV*). *B*, after DC101 treatment, more vessels in MCaIV stained for collagen IV. *C*, quantification of collagen IV coverage. Fractional coverage of collagen IV vessels was significantly higher in the DC101 group ($n = 6$ in control group, $n = 5$ in DC101-treated group; $P < 0.05$). *D*, quantification of $\alpha$-smooth muscle actin ($\alpha$SMA)-positive cells in the tumor vasculature. Fractional coverage of $\alpha$SMA-positive cells was significantly higher in the DC101 group ($n = 4$; $P < 0.005$). *E*, there was no change in plasma oncotic pressure in MCaIV tumors in the DC101 group when compared with the control group. However, the interstitial oncotic pressure dropped significantly in the DC101 group ($n = 5$; $P < 0.05$). *F*, DC101 did not affect the microvascular pressure (MVP), whereas the interstitial fluid pressure (IFP) was significantly reduced in MCaIV tumors ($n = 5$; $P < 0.05$). Thus, DC101 induced a hydrostatic pressure gradient across the vascular wall. Image width: *A* and *B*, 700 $\mu$m. Data are represented as mean ± SE.

DC101-induced decrease in IFP might be accompanied by a similar decrease in MVP. To test this, we measured MVP in control and DC101-treated tumors by directly inserting micropipettes in MCaIV tumor vessels (16). We found that MVP was unaffected by DC101 treatment (Fig. 3*F*). Thus, DC101 creates a sustained hydrostatic pressure gradient across the vasculature.

**DC101 Increases BSA Penetration in Tumors.** Movement of molecules across vessel walls occurs by diffusion and convection. Diffusion is governed by concentration gradients across the vessel wall, whereas convection is governed by pressure gradients. To test whether the pressure gradient across the vascular wall improves the penetration of large molecules, we injected fluorescently-labeled BSA i.v. into MCaIV-tumor-bearing mice and observed the pattern of BSA extravasation. We also identified functional blood vessels using biotinylated lectin. Quantitative analysis confirmed that DC101 produced a significantly deeper penetration of BSA molecules into the tumor (Fig. 4, *A–E*).

## Discussion

The data presented here provide compelling evidence in support of the normalization hypothesis: that judicious application of antiangiogenic treatment can normalize the tumor vasculature by pruning the immature vessels and fortifying the remaining ones (2). We show that the normalized tumor vasculature is less tortuous and the vessels are more uniformly covered by pericytes and basement membrane (Fig. 4*F*). This result implies that vessels with less mural cell coverage are more vulnerable to DC101-induced regression, which is consistent with previous findings that tumor vessels without mural cells tend to regress after VEGF withdrawal (21). Our functional data demonstrate for the first time that a drop in vascular permeability induces transvascular gradients in oncotic and hydrostatic pressure in tumors. The induced hydrostatic pressure gradient improves the penetration of large molecules into tumors.

In tumors, the abnormally high leakiness of the vasculature hinders drug delivery by inducing blood flow stasis (22, 23), whereas normalized vessels are less leaky to macromolecules. However, the permeability of the normalized vasculature is still significantly higher than that of normal tissues (12, 18). The small drop in oncotic pressure from 19 to 17 mm Hg induced by DC101 is also indirect evidence that the vascular permeability of DC101-treated MCaIV tumors is still elevated. For example, in s.c. tissue, the oncotic pressure is ~8 mm Hg (9). The change in oncotic pressure associated with DC101 leads to a minor increase in the hydrostatic pressure gradient, which is sufficient to increase the transvascular convection of a macromolecule and is most likely responsible for the deeper penetration of albumin.

Fluid movement across the vascular wall can be described by Starling's equation (18). Starling's equation states that the rate of fluid movement across a unit area of vascular wall ($J_v/A$) is proportional to the net pressure difference across the vessel wall:

$$J_v/A = L_p\{(MVP - IFP) - \sigma(\pi_p - \pi_i)\}$$

where $L_p$ (the hydraulic conductivity of the vessel wall) is the proportionality coefficient and A is the vascular wall area. As shown in the equation, the hydrostatic pressure gradient (MVP − IFP) is balanced by the oncotic pressure gradient [the difference between $\pi_p$ (plasma oncotic pressure) and $\pi_i$ (interstitial oncotic pressure)]. The reflection coefficient, $\sigma$, determines the effectiveness of the oncotic pressure gradient across the vascular wall. The value of $\sigma$ for albumin varies between 0 for the liver (with a high vascular permeability) and 1 for the impermeable brain vessels; lung has a $\sigma$ of 0.5 (24, 25). To our knowledge, the reflection coefficient of the tumor vasculature has

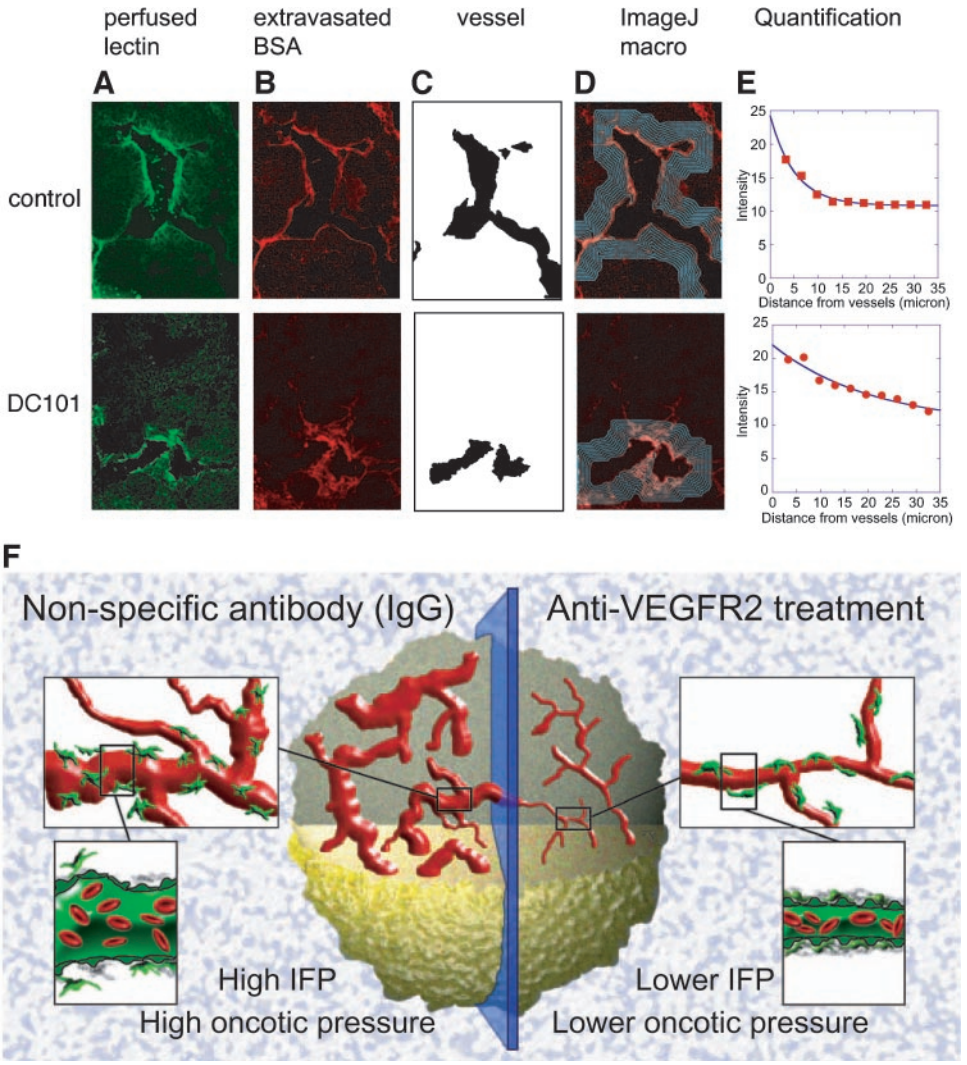


Fig. 4. Normalization of vessels improved the penetration of molecules in tumors. Mice bearing s.c. MCaIV tumors were injected with tetramethyl rhodamine isothiocyanate (TRITC)-BSA 1 h before perfusion fixation. Examples of frozen sections of MCaIV tumors with perfused biotinylated lectin (*A*) and extravasated TRITC-BSA (*B*) were prepared. Vessels were identified (*C*); and using an automated routine in ImageJ (http://rsb.info.nih.gov/ij/), we quantified the average intensity of extravasted TRITC-BSA as a function of distance from the blood vessel wall (*D* and *E*). The extravasation of BSA was quantified by fitting the intensity profiles to an exponential function to yield a characteristic penetration length ($n = 9$ sections; 3 sections per tumor; $P < 0.05$). The characteristic penetration lengths are 7.26 ± 1.11 $\mu$m (mean ± SE) and 11.23 ± 1.41 $\mu$m for the control and DC101 groups, respectively, indicating that DC101 leads to a more uniform penetration of albumin from blood vessels into the tumor. *F*, model of tumor vasculature normalization. Blood vessels in control tumors (treated with a nonspecific IgG antibody) are tortuous, hyperpermeable, and immature. Their high permeability and the lack of functional lymphatics lead to an elevated oncotic pressure and interstitial fluid pressure (*IFP*). DC101 (anti-VEGF receptor-2 treatment) prunes immature blood vessels and decreases the diameter of residual vessels; the vasculature becomes less tortuous and more organized, with more perivascular cells and basement membrane coverage. Furthermore, DC101 decreases vascular permeability, which induces a hydrostatic pressure gradient that improves drug delivery. Image width: *A–D*, 250 $\mu$m.

not been measured. Because the tumor vasculature has relatively large pores (26) and the oncotic pressure in the interstitium is similar to the oncotic pressure of plasma, the reflection coefficient is most likely close to 0. Based on the theory for hindered transport of rigid solutes, the calculated reflection coefficient for BSA is 0.0002 ($\sigma = [1 - [1 -$ radius of BSA (3.5 nm)/vessel pore size (500 nm)]$^2$]$^2$) (26). Thus, the increase in oncotic pressure gradient induced by DC101 has minimal effects on the transvascular flow.

We have previously shown that angiotensin II can increase the systemic blood pressure in mice and can create a pressure gradient across the vessel wall in tumors (20). Unfortunately, interstitial pressure catches up with vascular pressure, and the pressure gradient across the vessel wall dissipates in less than 1 min. Nevertheless, even these short-lived gradients can increase the delivery of specific antibodies in tumors (20). Thus, the sustained hydrostatic pressure gradient across the tumor vasculature, induced by DC101, can increase the transvascular convection of large molecules, despite a drop in vascular permeability to macromolecules.

The original rationale for combining antiangiogenic and cytotoxic therapies was to target two distinct cell populations within solid tumors: cancer cells and endothelial cells. When endothelial cells are targeted, blood vessels should be destroyed, and, thus, the delivery of therapeutics is compromised. However, several preclinical studies clearly demonstrate that the delivery of therapeutics is not compromised by antiangiogenic agents (27), and it even increases in some cases (28). The vessel normalization and the restoration of pressure gradients induced by VEGF blockade may explain the increased uptake of cytotoxic agents in tumors. For a cytotoxic agent to be effective, it must reach all cancer cells and in effective quantities. Antiangiogenic therapy, as shown by this study, might facilitate a more uniform delivery of therapeutic agents to cancer cells, including those that are farther from the vessels. This mechanism might contribute to the potentiation of conventional therapies by antiangiogenic agents (1, 10, 28–31).

## Addendum

To dissect molecular mechanisms involved in the normalization process, we collected total RNA and protein from MCaIV tumors 3 days after the completion of treatment with DC101 or control IgG. cDNA gene chips were used for screening (Angiogenic Gene Array, SuperArray, Bethesda, Maryland). Based on the gene array data, multiple genes were found to be differentially expressed after DC101 treatment (e.g. 2.2 fold downregulation of Ang2). Real time PCR data (LUX system, InVitrogen, Carlsbad, California) only confirmed the significant difference ($P < 0.005$) in Ang2 expression between control (n = 8, 1.29 ± 0.22) and DC101-treated group (n = 8, 0.29 ± 0.06). Furthermore, by Western analysis there was a marked decrease in the level of Ang2 protein after DC101 treatment. Immunostaining revealed Ang2 expression in both tumor and stromal cells. These data suggest that VEGFR2 blockade induces a decrease in Ang2 expression in tumors. Ang2 has been shown to destabilize blood vessel (7), thus the reduction in Ang2 expression may contribute to a more stable vasculature as described above. Further studies

are needed to understand the crosstalk between the VEGF and angiopoietin pathways.

## Acknowledgments

We thank Eugene M. Renkin (University of California Davis, Davis, CA) for his generous gift of the nylon wick material for interstitial fluid collection; T. Padera for lymphatic vessel endothelial hyaluronan receptor-1 (LYVE-1) staining; R. Delgiacco, P. Huang, J. Kahn, S. Roberge, and C. Smith for the outstanding technical support; S. Kwei for image analysis; M. Booth, E. Brown, W. Deen, D. Duda, D. Fukumura, R. Jones, L. Munn, J. Samson, M. Stohrer, E. di Tomaso, and J. Yuen for helpful comments.

## References

1. McCarthy M. Antiangiogenesis drug promising for metastatic colorectal cancer. Lancet 2003;361:1959.
2. Jain RK. Normalizing tumor vasculature with anti-angiogenic therapy: a new paradigm for combination therapy. Nat Med 2001;7:987–9.
3. Lee CG, Heijn M, di Tomaso E, et al. Anti-vascular endothelial growth factor treatment augments tumor radiation response under normoxic or hypoxic conditions. Cancer Res 2000;60:5565–70.
4. Willett CG, Boucher Y, Di Tomaso E, et al. Direct evidence that the VEGF-specific antibody bevacizumab has antivascular effects in human rectal cancer. Nat Med 2004;10:145–7.
5. Leu AJ, Berk DA, Lymboussaki A, Alitalo K, Jain RK. Absence of functional lymphatics within a murine sarcoma: a molecular and functional evaluation. Cancer Res 2000;60:4324–7.
6. Padera TP, Kadambi A, di Tomaso E, et al. Lymphatic metastasis in the absence of functional intratumor lymphatics. Science (Wash DC) 2002;296:1883–6.
7. Jain RK. Molecular regulation of vessel maturation. Nat Med 2003;9:685–93.
8. Boucher Y, Jain RK. Microvascular pressure is the principal driving force for interstitial hypertension in solid tumors: implications for vascular collapse. Cancer Res 1992;52:5110–4.
9. Stohrer M, Boucher Y, Stangassinger M, Jain RK. Oncotic pressure in solid tumors is elevated. Cancer Res 2000;60:4251–5.
10. Kozin SV, Boucher Y, Hicklin DJ, Bohlen P, Jain RK, Suit HD. Vascular endothelial growth factor receptor-2-blocking antibody potentiates radiation-induced long-term control of human tumor xenografts. Cancer Res 2001;61:39–44.
11. Brown EB, Campbell RB, Tsuzuki Y, et al. In vivo measurement of gene expression, angiogenesis and physiological function in tumors using multiphoton laser scanning microscopy. Nat Med 2001;7:864–8.
12. Yuan F, Chen Y, Dellian M, Safabakhsh N, Ferrara N, Jain RK. Time-dependent vascular regression and permeability changes in established human tumor xenografts induced by an anti-vascular endothelial growth factor/vascular permeability factor antibody. Proc Natl Acad Sci USA 1996;93:14765–70.
13. Morikawa S, Baluk P, Kaidoh T, Haskell A, Jain RK, McDonald DM. Abnormalities in pericytes on blood vessels and endothelial sprouts in tumors. Am J Pathol 2002;160:985–1000.
14. Boucher Y, Kirkwood JM, Opacic D, Desantis M, Jain RK. Interstitial hypertension in superficial metastatic melanomas in humans. Cancer Res 1991;51:6691–4.
15. Leunig M, Yuan F, Menger MD, et al. Angiogenesis, microvascular architecture, microhemodynamics, and interstitial fluid pressure during early growth of human adenocarcinoma LS174T in SCID mice. Cancer Res 1992;52:6553–60.
16. Peters W, Teixeira M, Intaglietta M, Gross JF. Microcirculatory studies in rat mammary carcinoma. I. Transparent chamber method, development of microvasculature, and pressures in tumor vessels J Natl Cancer Inst (Bethesda) 1980;65:631–42.
17. Abramsson A, Lindblom P, Betsholtz C. Endothelial and nonendothelial sources of PDGF-B regulate pericyte recruitment and influence vascular pattern formation in tumors. J Clin Investig 2003;112:1142–51.
18. Jain RK. Transport of molecules across tumor vasculature. Cancer Metastasis Rev 1987;6:559–93.
19. Dvorak HF, Nagy JA, Feng D, Dvorak HF. Tumor architecture and targeted delivery. In: Abrams PG, Fritzberg AR, editors. Radioimmunotherapy of cancer. New York: Marcel Dekker; 2002. p. 107–35.
20. Netti PA, Hamberg LM, Babich JW, et al. Enhancement of fluid filtration across tumor vessels: implication for delivery of macromolecules. Proc Natl Acad Sci USA 1999;96:3137–42.
21. Benjamin LE, Golijanin D, Itin A, Pode D, Keshet E. Selective ablation of immature blood vessels in established human tumors follows vascular endothelial growth factor withdrawal. J Clin Investig 1999;103:159–65.
22. Netti PA, Roberge S, Boucher Y, Baxter LT, Jain RK. Effect of transvascular fluid exchange on pressure-flow relationship in tumors: a proposed mechanism for tumor blood flow heterogeneity. Microvasc Res 1996;52:27–46.
23. Baish JW, Netti PA, Jain RK. Transmural coupling of fluid flow in microcirculatory network and interstitium in tumors. Microvasc Res 1997;53:128–41.
24. Parker JC, Perry MA, Taylor AE. Permeability of the microvascular barrier. In: Staub NC, Taylor AE, editors. Edema. New York: Raven Press; 1984. p. 143–87.
25. Aukland K, Reed RK. Interstitial-lymphatic mechanisms in the control of extracellular fluid volume. Physiol Rev 1993;73:1–78.
26. Hobbs SK, Monsky WL, Yuan F, et al. Regulation of transport pathways in tumor vessels: role of tumor type and microenvironment. Proc Natl Acad Sci USA 1998; 95:4607–12.
27. Wildiers H, Guetens G, De Boeck G, et al. Effect of antivascular endothelial growth factor treatment on the intratumoral uptake of CPT-11. Br J Cancer 2003;88:1979–86.
28. Teicher BA. A systems approach to cancer therapy. (Antioncogenics + standard cytotoxics → mechanism(s) of interaction). Cancer Metastasis Rev 1996;15:247–72.
29. Browder T, Butterfield CE, Kraling BM, et al. Antiangiogenic scheduling of chemotherapy improves efficacy against experimental drug-resistant cancer. Cancer Res 2000;60:1878–86.
30. Klement G, Baruchel S, Rak J, et al. Continuous low-dose therapy with vinblastine and VEGF receptor-2 antibody induces sustained tumor regression without overt toxicity. J Clin Investig 2000;105:R15–24.
31. Baker CH, Solorzano CC, Fidler IJ. Blockade of vascular endothelial growth factor receptor and epidermal growth factor receptor signaling for therapy of metastatic human pancreatic cancer. Cancer Res 2002;62:1996–2003.

# Vascular Normalization by Vascular Endothelial Growth Factor Receptor 2 Blockade Induces a Pressure Gradient Across the Vasculature and Improves Drug Penetration in Tumors

Ricky T. Tong, Yves Boucher, Sergey V. Kozin, et al.

*Cancer Res* 2004;64:3731-3736.